

WHY MEASURE NEW SNOW DENSITY, PRECIPITATION AND AIR TEMPERATURE?

H. Conway¹ and C. Wilbour

Geophysics Program, University of Washington and Washington State Department
of Transportation, Snoqualmie Pass

Abstract: The evolution of snow slope stability during storms is investigated using simple models to calculate the shear strength of a buried layer (from its density) and the imposed shear stress (from the weight of the overburden). There is a competition between the rate of loading from new snowfall and the rate of strengthening of buried layers. In theory, unstable conditions will occur when the stability index $\Sigma_z(t)$ (the ratio of the shear strength of a buried weak layer at depth z to the shear stress imposed by the overburden) approaches 1.0. A related index of practical interest is the expected time to failure (the time when $\Sigma_z(t)$ will become critical if the current conditions continue). The model is tested using measurements and observations of avalanche activity during three storm cycles at Snoqualmie Pass in the Washington Cascades. In two cases the avalanche activity was high while in the other, few avalanches released. $T_f(t)$ proved to be a better discriminator between stable and unstable conditions than $\Sigma_z(t)$. This is because it contains information about both the *magnitude* and the expected *changes* of $\Sigma_z(t)$ in response to the current conditions. Even if $\Sigma_z(t)$ is close to critical, if it is not decreasing then slopes will remain stable. Results indicate the model may prove useful for forecasting avalanches during storms. The required input (hourly measurements of precipitation, air temperature and new snow density) is routinely measured at many study sites and the tractability of the model makes it attractive for operational use.

Keywords

Storm and avalanche cycles, snow slope stability.

1. Introduction

Observations indicate that most natural dry snow slab avalanches release as a result of rapid loading from snowfall [McClung and Schaerer, 1993]. Here we examine the evolution of snow slope stability during storms. Of particular interest is to determine the conditions that cause these direct-action avalanches.

It is thought that the probability of slope failure increases when the stability index Σ_z (the ratio of the shear strength of a buried weak layer at depth z to the shear stress imposed by the overburden) approaches 1.0 [Perla and LaChapelle, 1970]. This has led to the continued popularity of field tests such as the Rutschblock [e.g., Fohn, 1987; Jamieson and Johnson, 1993a] or the shovel shear test [e.g., Schaerer, 1989; Jamieson and Johnson, 1993b] which yield an indication of the strength of

a buried weak layer relative to the stress from the overburden. There is a strong motivation to improve predictions of snow slope stability. Here we do not attempt a rigorous analysis of the coupled thermal-mechanical conditions expected in snow slabs, but rather we investigate the evolution of the strength of buried weak layers and the applied static stress from the overburden during storms. Our goal is to find an *index* that can be used as a tool in operational avalanche forecasting.

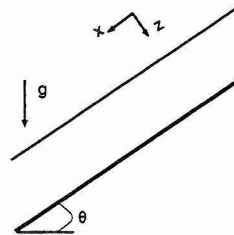


Figure 1. Coordinate convention used for planar snow slab inclined at angle θ .

¹Corresponding author address: H. Conway, Geophysics
Box 351650, University of Washington, Seattle, WA 98195.
tel: 206-685-8085, conway@geophys.washington.edu

2. Evolution of the stability index

2.1 Basal shear stress

Neglecting longitudinal stresses, the average static shear stress $\sigma_{zz}(t)$ at depth z and time t in a planar slab inclined at angle θ (Fig. 1) during times of precipitation is:

$$\sigma_{zz}(t) = g \int P_w \cos\theta \sin\theta dt \quad (1)$$

where the gravitational constant $g = 9.8 \text{ m s}^{-2}$ and P_w is the rate of accumulation (measured in the earth vertical direction). In theory, gauge measurements of precipitation from a representative site could be used in Eqn. 1, but in practice, interactions between winds and complex topography make it difficult to accurately predict the spatial and temporal pattern of accumulation.

2.2 Basal shear strength

Estimating the shear strength of a buried weak layer is also problematic. The mechanical properties of snow depend strongly on microstructure [Keeler, 1969; Hansen and Brown, 1987] but the relevant microstructural properties are generally not known nor measured. Although not ideal, bulk density is more easily (and more often) measured and mechanical properties undergo significant improvement with densification. From theory [Gibson and Ashby, 1987] and measurements [Perla et al., 1982; Jamieson, 1995], we approximate the shear fracture strength σ_f of snow of density ρ_s by:

$$\sigma_f = A \left(\frac{\rho_s}{\rho_i} \right)^2 \quad (2)$$

where $\rho_i = 917 \text{ kg m}^{-3}$ and $A = 1.95 \times 10^4 \text{ Pa}$.

Both metamorphic processes and the stress from the overburden $\sigma_{zz}(t)$ contribute to cause the density of a dry snow layer to change during a storm cycle. It is convenient to think of the metamorphic component as a stress $\sigma_m(t)$ that simply adds to the gravitational stress and assume a viscous densification law for dry snow of density $\rho_z(t)$ at depth z of the form:

$$\frac{1}{\rho_z(t)} \frac{d\rho_z}{dt} = \frac{1}{\eta_{zz}(t)} [\sigma_m(t) + \sigma_{zz}(t)] \quad (3)$$

Eqn. 3 applies to a horizontal snowpack but here we neglect the effect of shear on densification and apply the same expression for inclined snowpacks using $\sigma_{zz}(t) = g \int P_w \cos^2\theta dt$. The kinetic term $\eta_{zz}(t)$ is the compactive viscosity often used to represent a viscous constitutive relationship for dry snow [e.g.,

Kojima, 1967], modified with an Arrhenius type temperature term:

$$\eta_{zz}(t) = B_1 e^{B_2 \left(\frac{\rho_z(t)}{\rho_i} \right)} e^{E/(RT_z)} \quad (4)$$

When $B_1 = 6.5 \times 10^{-7} \text{ Pa s}$, $B_2 = 19.3$, the activation energy $E = 67.3 \text{ kJ mol}^{-1}$, the gas constant $R = 0.0083 \text{ kJ mol}^{-1} \text{ }^\circ\text{K}^{-1}$, the layer temperature T_z is in $^\circ\text{K}$, then η_{zz} is in units of Pa s.

We expect values of $\sigma_m(t)$ will range from being positive (equilibrium metamorphism) to negative under large temperature gradients (kinetic growth metamorphism). During storms we expect conditions are more conducive for equilibrium metamorphism and use a constant value (75 Pa) which is the average found from compaction measurements near the surface where $\sigma_{zz}(t) \approx 0$ [Marshall et al., submitted]. Using $\sigma_m = 75 \text{ Pa}$ implies that densification is dominated by metamorphic processes near the surface, but the gravitational component controls in layers more than 5 to 10 cm below the surface.

2.3 Stability index and time to failure

The average stability index $\bar{\Sigma}_z(t)$ at depth z and time t is:

$$\bar{\Sigma}_z(t) = \frac{\sigma_{fz}(t)}{\sigma_{zz}(t)} \quad (5)$$

$\sigma_{zz}(t)$ comes from Eqn. 1 and we solve for $\rho_z(t)$ iteratively (Eqns. 3 and 4) and use these in Eqn. 2 to calculate $\sigma_{fz}(t)$.

Of special interest for operational purposes is the expected time to failure $T_f(t)$ which is:

$$T_f(t) = \frac{(\bar{\Sigma}_z(t) - 1.0)}{d\bar{\Sigma}_z/dt} \quad (6)$$

$T_f(t)$ contains information about how the current conditions are affecting $\bar{\Sigma}_z(t)$ and when it will reach its critical value.

2.4 Sensitivity studies

The rate of densification (and hence strengthening) of a buried layer increases with load from the overburden (Eqn. 3). Although the snow is weakest immediately after deposition, the overburden stress is small which makes $\bar{\Sigma}_z(t)$ large. There is a competition between the rate of loading from new snowfall and the rate of strengthening of the basal layer. The basal layer strengthens more slowly at low rates of precipitation (because σ_{zz} is smaller) but if too low, the rate of loading will not exceed the rate of strengthening.

Fig. 2 shows the evolution of basal shear strength (initial density is 70 kg m^{-3} and T_z is $270 \text{ }^\circ\text{K}$ or

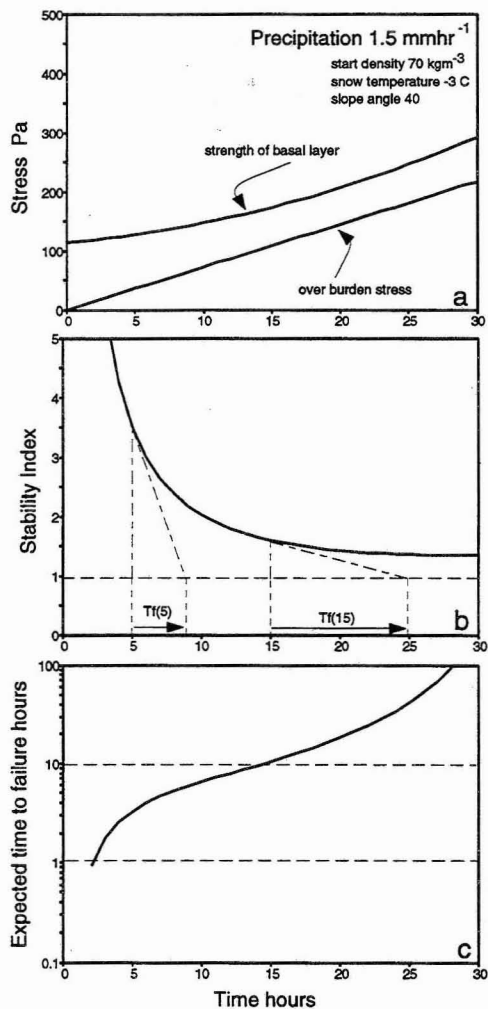


Figure 2. Evolution of stress, strength, stability index and expected time to failure calculated for constant precipitation of 1.5 mm hr^{-1} . Other initial conditions are given in the figure. In this case the model predicts stable conditions.

-3°C) and shear stress calculated for (constant) precipitation of 1.5 mm hr^{-1} . Also shown is the stability index $\bar{\Sigma}_z(t)$ (Fig. 2b) which decreases slowly to a minimum of ~ 1.3 , but then increases after 35 hours (not shown). The figure also shows a graphical representation of the expected time to failure after 5 hours ($T_f(5) = 3.3 \text{ hrs}$) and after 15 hours ($T_f(15) = 10.5 \text{ hrs}$).

A continuous plot of $T_f(t)$ is shown in Fig. 2c - note the log scale. Initially $T_f(t)$ is short (Fig. 2c) but we do not expect hazardous avalanches then because the slab thickness is only $\sim 3 \text{ cm}$. $T_f(t)$ increases with time ($T_f(30) > 100$). The model predicts 40° slopes will remain stable.

Fig. 3 is a plot for constant precipitation of 2.5 mm hr^{-1} but otherwise the same conditions as

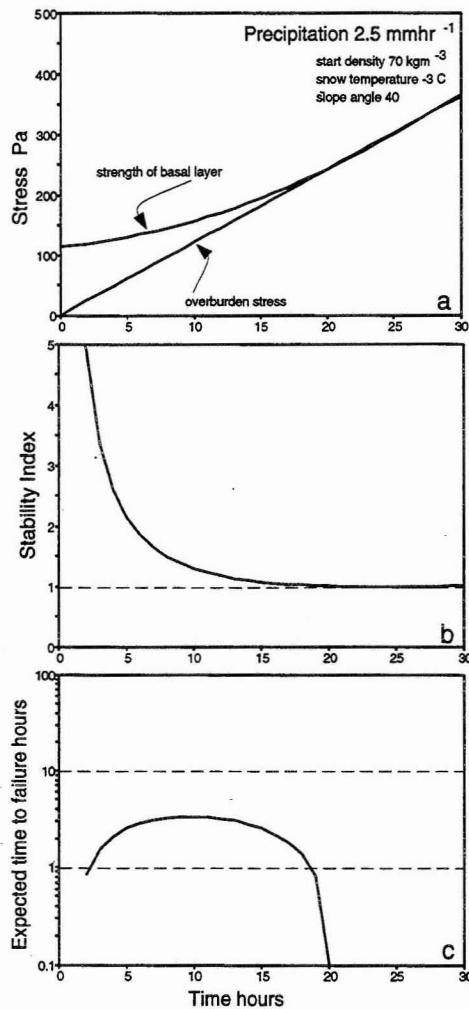


Figure 3. Evolution of stress, strength, stability index and expected time to failure calculated for (constant) precipitation of 2.5 mm hr^{-1} . Other initial conditions are given in the figure. In this case the model predicts failure after 21 hours.

Fig. 2. $\bar{\Sigma}_z(t)$ decreases rapidly in the first 5 hours and then more slowly to a minimum value less than 1.0 after 21 hours. The expected time to failure is about 2-3 hours for the first 15 hours, but $T_f(t)$ decreases rapidly in the last 2 hours as $\bar{\Sigma}_z(t) \rightarrow 1.0$. Failure of 40° slopes is predicted after 21 hours.

3. Model application - case studies

Observations of precipitation, new snow density, air temperature and avalanche activity from the Washington Cascades near Snoqualmie Pass, U.S.A. are used to test the model. The terrain near Snoqualmie Pass lies between 900 m and 1700 m. The region has a maritime climate and storms often deposit up to 1 m of new snow. Direct action avalanches are common and have a major impact

on winter travellers along the Interstate 90 highway.

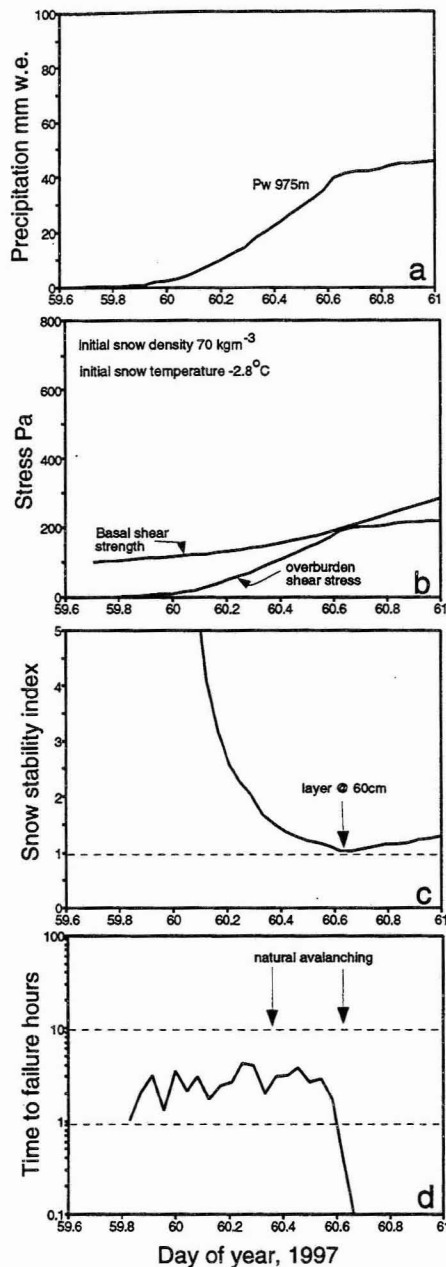


Figure 4. Measurements of cumulative precipitation at 975 m starting at 1500 hrs on February 28, 1997 (day 59.625). Also shown is the strength of the basal layer and the shear stress from the overburden for a 40° slope (b), the average stability index $\bar{\Sigma}_z(t)$ at the basal layer (c), and the expected time to failure $T_f(t)$ (d).

Measurements of new snow density at the Department of Transportation study plot (915 m a.s.l.) are used to calculate the initial strength of the new snow (Eqn. 2). A full energy balance is beyond the scope of this work and instead we assume the layer tem-

perature is the same as the air temperature at the time of deposition. This approximation breaks down during times of rapid warming or rain when heat can be advected rapidly into the snowpack but is reasonable over short time-scales during times of snowfall. Hourly measurements of precipitation from a heated gauge either at the study plot or at a local ski area were used to calculate $\sigma_{zz}(t)$ and $\sigma_{xz}(t)$ for slopes of 40° and then used in Eqns. 3 and 4 to calculate the evolution of shear strength, shear stress, stability index, and expected time to failure.

3.1 Storm cycle of March 1, 1997

An avalanche cycle at Snoqualmie Pass on March 1, 1997 closed the I-90 highway for about 24 hours. Small slides consisting of just the recent storm snow first released early in the morning when the highway was still open. A car and a road grader were caught in a natural avalanche at the East Snowshed. No people were injured. Although the grader was able to drive out of the debris, the car could not be extracted safely and it was subsequently buried by controlled avalanches. Stephanie Breyfogle (her husband Steve is well known for his presentations at past Snow Science Workshops) ran into a natural avalanche crossing the highway. She was rear ended by a following car, which was rear ended by a plow truck. A second truck veered to the side to miss the cars and ran into the avalanche. Two State Patrolmen were caught and partly buried, and 3 more cars that were backed up by the incidents were partially buried by a second avalanche. At about 1030 hrs an avalanche hit a house in the Alpental village and buried it above the third floor window. The same house and another about 100 m away was hit again at about 1500 hrs. The avalanches released from slopes above that had been recently logged. An 11 year old out of bounds skier was caught in an avalanche that swept him through trees and over a cliff. He stopped about 15 m from the highway, alive but without his equipment.

Fig. 4a shows measurements of cumulative precipitation at 975 m starting at 1500 hrs on February 28, 1997 (day 59.625). Measurements at 600 hrs on March 1 indicated 20 cm of new, low density snow ($\rho_0(0) = 70 \text{ kg m}^{-3}$, $T_s = -2.8^\circ\text{C}$). High intensity snowfall (up to 17 mm hr^{-1}) and natural avalanche activity continued through the afternoon. Fig. 4b shows the strength of the basal layer and the shear stress from the overburden (for a 40° slope), and Fig. 4c shows the evolution of the stability index. $\bar{\Sigma}_z(t) = 1.3$ when avalanche activity first started and $\bar{\Sigma}_z(t) < 1.0$ at 1500 hrs when the basal layer was $\sim 60 \text{ cm}$ below the surface. We are not certain

that the measurements in the study plot are representative of conditions in the starting zones and additional calculations indicate that if $\rho_0(0)$ was 10% lower and the local precipitation was 20% higher than measured at the study site, $\bar{\Sigma}_z(t) < 1.0$ at 1100 hrs.

Fig. 4d shows the expected time to failure varied from ~ 2 to 3 hours for most of the storm. $T_f(t)$ decreased rapidly to zero at 1500 hrs when $\bar{\Sigma}_z(t) < 1.0$.

3.2 Storm cycle of February 5, 1996

A major avalanche cycle at Snoqualmie Pass on February 5, 1996 closed the I-90 highway for 44 hours. Cars and people were caught and buried by several direct action avalanches prior to a classic warm-up and rain. One traveller who was out of his car was buried about 2 m below the surface for 29 minutes before being found by probing and dug out alive. Avalanches hit and partially buried a snow blower and a vehicle occupied by two avalanche technicians who were spotting for the blower. In all, 11 vehicles and at least 20 people were hit by avalanches; more were dusted.

Fig. 5a shows measurements of precipitation starting at noon on day 34 (February 3). By next morning 12 cm of new snow ($\rho_0(0) = 120 \text{ kg m}^{-3}$, $T_s = -15.3^\circ\text{C}$) had accumulated but avalanche activity was minor. The weather cleared in the afternoon but precipitation started again in the morning of day 36 (February 5). Avalanches first ran naturally at 1730 hrs, releasing as slabs about 20 cm deep. Precipitation changed to rain at 1900 hrs.

Fig. 5b shows the strength of the basal layer and the shear stress from the overburden (for a 40° slope), and Fig. 5c shows the stability index at the basal layer and at a layer deposited early in the morning of February 5 (day 36.04 - $\rho_0(0) = 110 \text{ kg m}^{-3}$, $T_s = -9.8^\circ\text{C}$). $\bar{\Sigma}_z(t) = 1.6$ at the basal layer $\sim 20 \text{ cm}$ below the surface when avalanching first started. The index was higher ($\bar{\Sigma}_z(t) = 1.8$) 13 cm below the surface. However the index decreased rapidly during the evening and just prior to rain $\bar{\Sigma}_z(t) = 1.4$ both at the basal layer (then about 32 cm below the surface) and at the layer 25 cm below the surface. The measurements of snow density are surprisingly high given the cold air temperatures at the time of deposition. Other things being equal we expect new snow densities more in the range 50 to 80 kg m^{-3} at these temperatures *LaChapelle* [1969]. It is likely that winds contributed to densify the new snow, but it is also possible that some of the new snow fell under conditions of little or no wind resulting in a buried thin, low density (weak) layer.

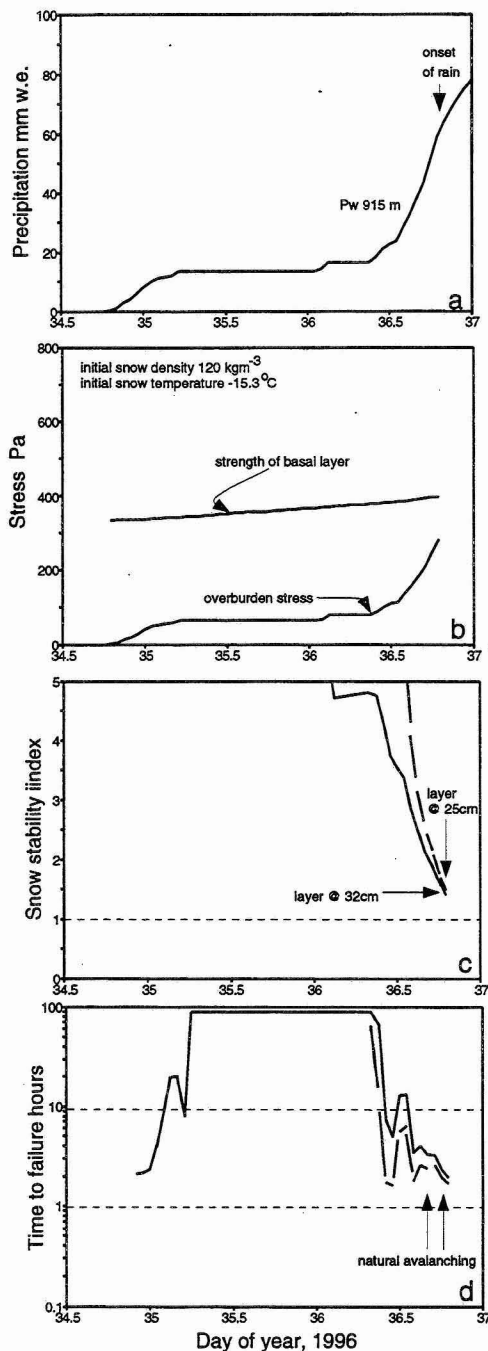


Figure 5. Measurements of cumulative precipitation at 915 m (a) starting at midday on February 3, 1996 (day 34.5). Also shown is the strength of the basal layer and the shear stress from the overburden for a 40° slope (b) the average stability index $\bar{\Sigma}_z(t)$ at two depths (c), and the expected time to failure $T_f(t)$ at those two depths (d). Natural avalanches first ran naturally at 1730 hrs on February 5.

Model calculations indicate that an initial density of 80 kg m^{-3} (rather than 110 kg m^{-3} measured) would cause $\bar{\Sigma}_z(t) < 1.0$ at 1700 hrs - about the time of the

onset of avalanching.

Fig. 5d shows the expected time to failure decreased rapidly to less than 2 hours shortly before the onset of avalanching. $T_f(t)$ remained low until rain started.

3.3 Storm cycle of January 8-15, 1989

More than 1.25 m of snow accumulated during the week of January 8-15, 1989, but no natural avalanches were observed until rain started late on January 15. Avalanche control with explosives during the storm released a few small avalanches but despite the large accumulation of snow, activity was minor. Fig. 6a shows measurements of precipitation which started as snow ($\rho_0(0) = 90 \text{ kg m}^{-3}$, $T_s = -0.8^\circ\text{C}$) on January 13 and changed to rain at 1600 hrs on January 15.

Fig. 6b shows the basal shear strength and stress for a 40° slope, and Fig. 6c shows the evolution of the stability index at the basal layer and at a layer deposited early in the morning of day 14.0 ($\rho_0(0) = 95 \text{ kg m}^{-3}$, $T_s = -4.7^\circ\text{C}$). The minimum stability index at the basal layer (about 40 cm below the surface when rain started) was 1.7, but the minimum for the snowpack ($\bar{\Sigma}_z(t) = 1.5$) occurred $\sim 25 \text{ cm}$ below the surface just prior to rain. In this case it turns out that the stability index would increase for steeper slopes ($\bar{\Sigma}_z(t) = 1.6$ on slopes of 50°) but $\bar{\Sigma}_z(t) \rightarrow 1.0$ if the local precipitation was $1.75\times$ higher than the gauge measurement or if the initial density was 65 kg m^{-3} (rather than 95 kg m^{-3} measured). However we do not expect such a large enhancement of precipitation, nor such a low initial density.

Fig. 6d shows the expected time to failure of both layers was generally high and increasing during the storm. Even when the stability index was a minimum just prior to rain, T_f was more than 30 hours. Both the magnitude and the increasing trend distinguish the T_f curve from those observed in the other two storms.

4. Discussion

4.1 Does the model predict instability?

We are not certain what value $\bar{\Sigma}_{zc}$ is critical for slope stability. Although encouraging that the stability index was lower during storms when avalanche activity was intense ($\bar{\Sigma}_z = 1.4$ compared to 1.5), analysis of the uncertainties and a standard t-test indicates the two values are not significantly different.

Results suggest $T_f(t)$ discriminates much more clearly between stable and unstable conditions than

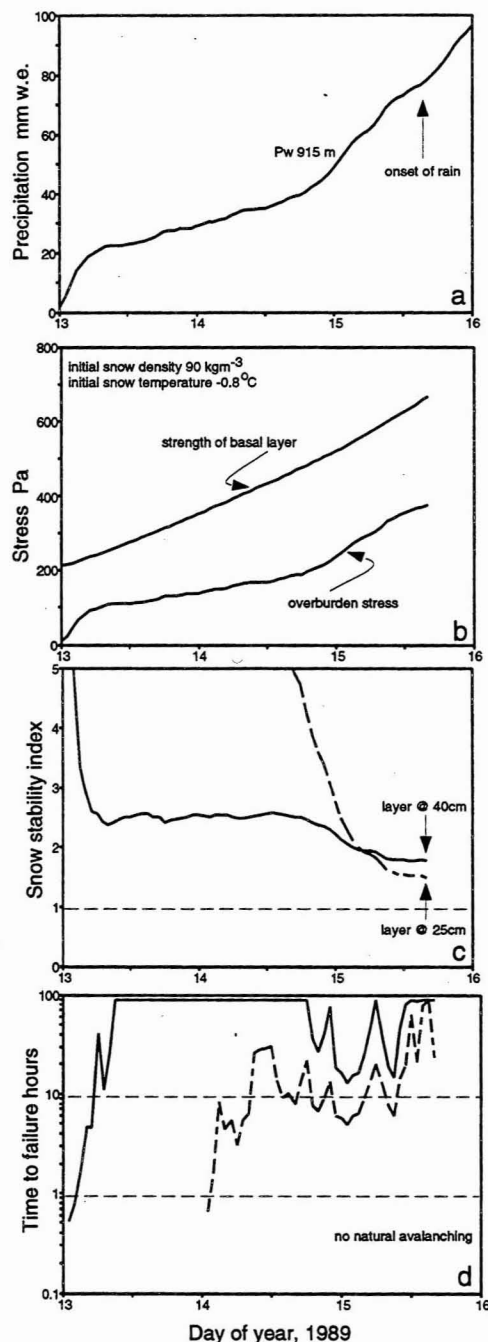


Figure 6. Measurements of cumulative precipitation at 915 m (a) starting on January 13, 1989. Also shown is the strength of the basal layer and the shear stress from the overburden for a 40° slope (b), the average stability index $\bar{\Sigma}_z(t)$ calculated at two depths (c), and the expected time to failure $T_f(t)$ at those two depths (d). Few natural avalanches released during this storm

$\bar{\Sigma}_z(t)$. $T_f(t)$ was more than an order of magnitude lower during storms when avalanche activity was intense ($T_f(t) = 2 \text{ cf. } 20 \text{ hrs}$). This is because $T_f(t)$

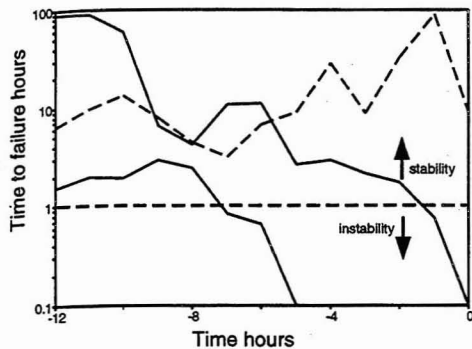


Figure 7. Expected time of failure recalculated for the three storms discussed previously assuming instability if $\bar{\Sigma}_{zc} = 1.4$.

contains information about both the *magnitude* and the expected *changes* of $\Sigma_z(t)$ under the current conditions. Even if $\Sigma_z(t)$ is close to critical, slopes are expected to remain stable if it is not converging to its critical value.

More case histories are needed to further develop and refine the model. For example results above suggest slope stability may be critical if $\bar{\Sigma}_{zc} \leq 1.4$ (rather than 1.0). Fig. 7 shows $T_f(t)$ for the three storms recalculated with $\bar{\Sigma}_{zc} = 1.4$. Using this criterion we might expect instability when $T_f(t)$ is less than ~ 1.0 hour.

4.2 Model limitations

We emphasise that the model is a *tool* that may prove useful for evaluating snow slope stability during storms. Values derived from the model should be treated with caution. For example σ_f is an index of the *elastic fracture* strength - higher values are expected at lower strain rates or warmer temperatures [McClung, 1977, 1996]. Here we do not consider the critical strain rate condition that must also be met before failure will occur [e.g., McClung, 1981; Narita, 1983; Gubler and Bader, 1989; Bader and Salm, 1990].

We caution that the model is sensitive to the initial density of the new snow. More measurements are needed to improve the strength/density parameterization and also to improve the densification law. Although a full energy balance to model snow temperature may improve the densification law, for the short time scales of interest here, we suspect that changes in layer temperature has a small effect compared to other uncertainties. We also emphasise that the analysis is not rigorous in that we do not account for effects such as stress concentrations that would cause local stresses to be higher than the average used here, or longitudinal stresses which would act

in the opposite sense providing support for the slab. Inclusion of these effects would undoubtedly improve the model but would reduce its tractability.

4.2 Model application

The simple model can be easily incorporated into an operational forecasting system using standard measurements of air temperature and precipitation for input. Currently the model also requires the new snow density as input but we are investigating parameterizations of new snow density using standard meteorological measurements.

5. Conclusions

Relatively simple parameterizations of the shear strength of buried layers and the imposed loading from the weight of the overburden offer a means to examine the evolution of snow slope stability during storms. In particular, unstable conditions are expected when the stability index $\Sigma_z(t)$ (the ratio of the shear strength of a buried weak layer at depth z to the shear stress imposed by the overburden) approaches 1.0. A related index $T_f(t)$ is the time expected to failure which takes into account both the *magnitude* and the expected *changes* of $\Sigma_z(t)$ in response to the current conditions.

Comparison of model results with measurements and observations during three storm cycles indicates $T_f(t)$ provides a particularly useful discriminator between stable and unstable conditions. Given the model assumptions and associated large uncertainties, the model does surprisingly well at predicting slope stability using standard measurements of new snow density, precipitation and air temperature.

References

- Bader, H.-P., and B. Salm, On the mechanics of snow slab release, *Cold Regions Science and Technology*, 17, 287-300, 1990.
- Fohn, P. M. B., The Rutschlock as a practical tool for slope stability evaluation, in *Avalanche Movement and Effects. Proc., Davos Symposium*, no. 162, pp. 223-228, Int. Ass. Hydrol. Sci., 1987.
- Gibson, L. J., and M. F. Ashby, *Cellular solids. Structure and properties*, Pergamon Press, New York, 1987, 336 pp.
- Gubler, H., and H.-P. Bader, A model of initial failure in slab-avalanche release, *Ann. Glaciol.*, 13, 90-95, 1989.
- Hansen, A. C., and R. L. Brown, A new constitutive theory for snow based on a micro-mechanical approach, in *Avalanche Movement and Effects. Proc. Davos Symposium*, no. 162, pp. 87-104, Int. Ass. Hydrol. Sci., 1987.

- Jamieson, J. B., Avalanche prediction for persistent snow slabs, Ph.D. thesis, Dept. Civil Eng., Univ. Calgary, Alberta, Canada, 1995, 258pp.
- Jamieson, J. B., and C. D. Johnson, Rutschblock precision, technique variations and limitations, *J. Glaciol.*, 39(133), 666-674, 1993a.
- Jamieson, J. B., and C. D. Johnson, Shear frame stability parameters for large scale avalanche forecasting, *Ann. Glaciol.*, 18, 268-273, 1993b.
- Keeler, C. M., The growth of bonds and the increase of mechanical strength in a dry seasonal snow-pack, *J. Glaciol.*, 8(54), 441-450, 1969.
- Kojima, K., Densification of seasonal snowcover, in *Physics of Snow and Ice, Proc. Int. Conf. on Low Temp. Sci.*, edited by H. Oura, vol. 1, pp. 929-952, Hokkaido Univ., Sapporo, 1967.
- LaChapelle, E. R., Properties of snow. Paper prepared for Hydrologic Systems course presented by College of Forest Resources, University of Washington, Seattle, 21pp., 1969.
- Marshall, H. P., H. Conway, and L. A. Rasmussen, Snow densification during rain, *Cold Regions Science and Technology*, submitted.
- McClung, D. M., Direct simple shear stress tests on snow and their relation to slab avalanche formation, *J. Glaciol.*, 19(81), 101-109, 1977.
- McClung, D. M., Fracture mechanical models of dry slab avalanche release, *J. Geophys. Res.*, 86, 10783-10790, 1981.
- McClung, D. M., Effects of temperature on fracture in dry slab avalanche release, *J. Geophys. Res.*, 101, 21907-21920, 1996.
- McClung, D. M., and P. Schaerer, eds., *The Avalanche Handbook*, The Mountaineers, Seattle, WA., 1993, 271pp.
- Narita, H., An experimental study on tensile fracture of snow, *Low Temp. Science, Ser. A*, 32, 1-37, 1983.
- Perla, R., and E. LaChapelle, A theory of snow slab failure, *J. Geophys. Res.*, 75(36), 7619-7627, 1970.
- Perla, R., T. Beck, and T. Cheng, The shear strength index of alpine snow, *Cold Regions Science and Technology*, 6(1), 1982.
- Schaerer, P., Evaluation of the shovel shear test, in *Proceedings Int. Snow Sci. Workshop, Whistler, BC*, pp. 274-276, 1989.

Corresponding author address: H. Conway, Geophysics Box 351650, University of Washington, Seattle, WA 98195. tel: 206-685-8085, conway@geophys.washington.edu

This preprint was prepared with AGU's L^AT_EX macros v4, with the extension package 'AGU++' by P. W. Daly, version 1.5d from 1997/04/28.

Acknowledgments

This research was funded by the U.S. Army Research Office (Grant No. DAAH04-95-1-0172). We

also wish to thank the Washington State Department of Transportation for logistical support and Al Rasmussen for his assistance.